NAVAL POSTGRADUATE SCHOOL
Monterey, California

THESIS

Apparatus to Determine the Complex Mass of a Viscous Fluid Contained in a Rigid Porous Solid from Acoustic Pressure Measurements

by

Robert Allen Mirick

December 1989

Thesis Advisor: S. R. Baker
Co-advisor O. B. Wilson

Approved for public release; distribution unlimited.

UNCLASSIFIED

Security Classification of this page

REPORT DOCUMENTATION PAGE

1a Report Security Classification UNCLASSIFIED	1b Restrictive Markings
2a Security Classification Authority	3 Distribution Availability of Report: Approved for public release; distribution is unlimited.
2b Declassification/Downgrading Schedule	
4 Performing Organization Report Number(s)	5 Monitoring Organization Report Number(s)
6a Name of Performing Organization: Naval Postgraduate School; 6b Office Symbol (If Applicable): 3A	7a Name of Monitoring Organization: Naval Postgraduate School
6c Address (city, state, and ZIP code): Monterey, CA 93943-5000	7b Address (city, state, and ZIP code): Monterey, CA 93943-5000
8a Name of Funding/Sponsoring Organization 8b Office Symbol	9 Procurement Instrument Identification
8c Address (city, state, and ZIP code)	10 Source of Funding Numbers: Program Element Number; Project No; Task No; Work Unit Accession No

11 Title (Include Security Classification) APPARATUS TO DETERMINE THE COMPLEX MASS OF A VISCOUS FLUID CONTAINED IN A RIGID POROUS SOLID FROM ACOUSTIC PRESSURE MEASUREMENTS

12 Personal Author(s) Mirick, Robert A.

13a Type of Report	13b Time Covered	14 Date of Report (year, month,day)	15 Page Count
Master's Thesis	From To	1989 December	52

16 Supplementary Notation The views expressed in this thesis are those of the author and do not reflect the official policy or position of the Department of Defense or the U.S. Government.

17 Cosati Codes			18 Subject Terms (continue on reverse if necessary and identify by block number)
Field	Group	Subgroup	Acoustic Impedance, Acoustic Coupler, Complex Mass Density, Fluid Saturated, Porous Media

19 Abstract (continue on reverse if necessary and identify by block number)

Two experimental techniques to determine the frequency-dependent complex mass of a viscous fluid contained in a rigid porous solid are investigated. In one technique the moving mass of the fluid is sensed by its effect on the measured input electrical impedance of a moving coil transducer. In the second technique the moving mass is extracted from the measured acoustic pressure required for the fluid to oscillate with a known amplitude through the solid frame. A description of the apparatus and preliminary results using the pressure method as well as a comparison of the two techniques are presented.

20 Distribution/Availability of Abstract	21 Abstract Security Classification	
[X] unclassified/unlimited [ ] same as report [ ] DTIC users UNCLASSIFIED	UNCLASSIFIED	
22a Name of Responsible Individual: PROF. S. R. Baker	22b Telephone (Include Area code): (408) 646-2729	22c Office Symbol: 61BA

DD FORM 1473, 84 MAR 83 APR edition may be used until exhausted

All other editions are obsolete

security classification of this page UNCLASSIFIED

Approved for public release; distribution is unlimited.

Apparatus to Determine the Complex Mass of a Viscous Fluid Contained in a Rigid Porous Solid from Acoustic Pressure Measurements

by

Robert Allen Mirick
Lieutenant Commander, United States Navy
B. S., United States Naval Academy, 1979

Submitted in partial fulfillment of the
requirements for the degree of

MASTER OF SCIENCE IN ENGINEERING ACOUSTICS

from the

NAVAL POSTGRADUATE SCHOOL

December 1989

ABSTRACT

Two experimental techniques to determine the frequency-dependent complex mass of a viscous fluid contained in a rigid porous solid are investigated. In one technique the moving mass of the fluid is sensed by its effect on the measured input electrical impedance of a moving coil transducer. In the second technique the moving mass is extracted from the measured acoustic pressure required for the fluid to oscillate with a known amplitude through the solid frame. A description of the apparatus and preliminary results using the pressure method as well as a comparison of the two techniques are presented.

TABLE OF CONTENTS

ACKNOWLEDGEMENTS

I appreciate the support of the faculty, staff, and students of the Physics Department, Naval Postgraduate School. I thank Professors Baker and Wilson for their tutelage and guidance. This thesis represents a cherished personal and military professional achievement accomplished with encouragement and sacrifice on the part of my wife, Pam, and our children; Kristen, Kathryn, and Meredith.

I. INTRODUCTION

A. BACKGROUND

Acoustic propagation in the ocean is frequently controlled by the sea bottom (Urick, 1982, p. 11-1). Reflective bottom loss due to impedance mismatch, scattering due to bottom roughness, and attenuation due to dilitational and shear wave excitation in bottom sediment all dominate shallow water transmission at low frequencies, and influence deep water propagation to short and intermediate ranges at mid-frequencies (Tolstoy and Clay, 1972, p. 8). The importance of these physical phenomena to underwater acoustics is well recognized. Extensive literature is available on the broad subject of marine sediment acoustics because of the vast contributions by many renowned individuals over the past several decades, e.g., Hampton (1974), Hamilton (1974), Kuperman and Jensen (1980), Akal and Berkson (1986), and Stoll (1986).

Even so, one example of bottom interaction physics that remains difficult to specify theoretically and validate experimentally is the frequency dependence of the attenuation. Because of the difficulty of measuring attenuation at low frequencies, values are obtained by extrapolation from accurate high frequency measurements; too often decades removed from the frequency span of study (Hovem, 1980, p. 2). This problem, coupled with the inherent experimental

uncertainties and the fact that no single data set spans the entire frequency range of interest in underwater acoustics, i.e., Hz to MHz (Kibblewhite, 1989, p. 718), underscores the requirement for an accurate theoretical model for the attenuation of sound in sediments. Such a theoretical model can be prescribed by applying the Biot theory of acoustic wave propagation. Biot theory accounts for fluid-solid viscous interaction, which is an important ingredient in the phenomena of bottom attenuation. However, the details of this interaction are not well characterized for porous solid geometries.

The Biot model of fluid-saturated sediment contains thirteen parameters, defined in Biot (1956a,1956b), Stoll (1974,1985,1986), and Plona and Johnson (1984), which depend on the microscopic pore geometry of the porous solid, the bulk properties of the solid, and the bulk properties of the fluid. These parameters are very difficult to extract from conventional measurements of compressional sound speed and attenuation. This fact, along with the paucity of independent observations of the effects of fluid-solid interaction, has been one of the major obstacles to general acceptance of the Biot-Stoll view by the underwater acoustics community (Kibblewhite, 1989, p. 718). However, recent developments include success in defining some of the key Biot parameters and coefficients. As reported by Kibblewhite (1989); Bedford et al (1984), Johnson et al (1987), and Baker (1986) have contributed significantly to specifying parameters required as input to the Biot formulation of elastic wave propagation in a fluid saturated porous solid.

Least well known are the three parameters which depend on the microscopic pore geometry and which, along with the bulk fluid density, completely determine the so-called complex mass density, $\tilde{\rho}$, of the fluid in the pores (Ogushwitz, 1985, p.430, and Stoll, 1985, p.1798)(as revealed in Chapter II, the complex mass density for a rigid and stationary porous solid is the negative of the ratio of the gradient in fluid pressure to its acceleration). For this reason, a measurement of $\tilde{\rho}$ is a superior probe of these parameters (Baker, 1986, p. 2).

B. OBJECTIVES

The goal of this research program is to determine the frequency-dependent complex mass of a viscous fluid in a rigid and stationary porous solid for various typical pore geometries. Two experimental techniques are being investigated, with the fluid-saturated solid sample contained in a small cylindrical cavity, depicted in Fig. 1 (Grant, 1988, p. 4). The first technique, the so-called impedance method, is based on electroacoustic network theory. The moving mass of the fluid is sensed by the measured input electrical impedance of moving coil drivers. Preliminary results for the impedance method have been reported by LCDR Grant (Grant, 1988, p. 57). The second technique, the so-called direct method, is based on Newton's Second Law for a viscous fluid contained in a rigid porous solid. Stiff piezoceramic drivers are used to apply a known displacement for a

given voltage input. The moving mass is extracted from the observed pressure difference across the sample required for the pore fluid to oscillate with a known amplitude.

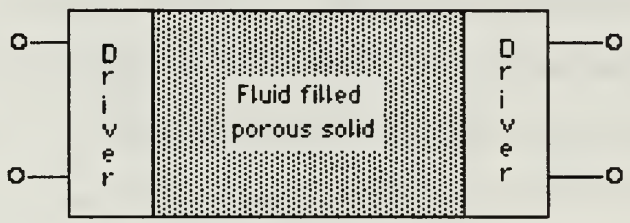

Figure 1. Simple Model.

The specific objectives of the research described in this thesis are: (1) to develop and calibrate an apparatus to extract the complex fluid mass contained in a rigid porous solid from acoustic pressure and particle velocity measurements (direct method), (2) to compare these calibration results with those of the impedance method (Grant, 1988, pp. 44-56), and (3) to identify the better method of the two for further investigation with various porous solid sample geometries.

II. THEORY

A. BIOT-STOLL THEORY OF SOUND PROPAGATION IN A FLUID-FILLED POROUS SOLID

As summarized by Stoll (1974), propagation of sound in the ocean bottom is mainly controlled by two fundamentally different mechanisms: the first is the friction at grain-grain contacts due to the inelasticity of the solid frame, and the second is the viscous drag between the pore fluid and solid frame. Sediments of low permeability also exhibit another kind of viscous damping, attributed to local fluid motion around intergranular contacts (Stoll, 1985, p. 1790).

In principle, the motion of solid and fluid components can be described by differential equations for a microscopic volume element of porous material, subject to the appropriate boundary conditions at the solid frame-pore fluid interface. Solutions to these equations can be found only if the microscopic pore geometry is completely specified, a practical impossibility. However, a phenomenological, macroscopic (averaged over the microscopic structure) description of motion is possible, as long as the acoustic wavelength is much greater than a characteristic pore radius. Biot derived just such a description of motion in his series of classic papers (Biot, 1956a, 1956b, 1962). Many equivalent formulations of Biot equations and parameters exist to

suit particular applications. My choice is the set of equations of motion presented by Baker (1986, p. 29):

$$\rho_1 \frac{\partial^2}{\partial t^2}\mathbf{u} = -\rho_a \frac{\partial^2}{\partial t^2}(\mathbf{u} - \mathbf{U}) + B\nabla(\nabla\cdot\mathbf{u}) + C\nabla(\nabla\cdot\mathbf{U}) - N\nabla\times\nabla\times\mathbf{u} - bF\frac{\partial}{\partial t}(\mathbf{u} - \mathbf{U}) \quad (2.1)$$

$$\rho_2 \frac{\partial^2}{\partial t^2}\mathbf{U} = -\rho_a \frac{\partial^2}{\partial t^2}(\mathbf{U} - \mathbf{u}) + C\nabla(\nabla\cdot\mathbf{u}) + D\nabla(\nabla\cdot\mathbf{U}) - bF\frac{\partial}{\partial t}(\mathbf{U} - \mathbf{u}) \quad (2.2)$$

where,

$\mathbf{U}$ = average fluid displacement,

$\mathbf{u}$ = average frame displacement,

ρ_1 = mass density of bulk solid multiplied by the volume fraction of solid, i.e., $\rho_1 = (1 - P)\rho_s$,

ρ_2 = mass density of bulk fluid multiplied by the volume fraction of fluid, i.e., $\rho_2 = P\rho_f$,

ρ_a = effective mass density normalized to the apparent fluid density, i.e., $\rho_a = (\alpha - 1)P\rho_f$,

P = porosity, defined as the volume fraction of fluid,

α = tortuosity parameter, a function of the microscopic pore geometry,

b = friction coefficient = PR_{DC} ; R_{DC} is the DC flow resistance, defined as the average gradient in fluid pressure divided by the average fluid velocity in the direction of $-\nabla p$,

N = shear modulus of the frame,

F = complex, frequency-dependent, universal correction function.

The coefficients B, C, and D are generalized elastic constants, and are functions of the bulk fluid and solid elastic contants, and the porosity, as follows:

$$B = \frac{\left[1 - P - \frac{K_b}{K_s}\right](1 - P)K_s + P\frac{K_s}{K_f}K_b}{\left[1 - P - \frac{K_b}{K_s}\right] + P\frac{K_s}{K_f}} + \frac{4}{3}N \qquad (2.3)$$

$$C = \frac{\left[1 - P - \frac{K_b}{K_s}\right]PK_s}{\left[1 - P - \frac{K_b}{K_s}\right] + P\frac{K_s}{K_f}} \qquad (2.4)$$

$$D = \frac{P^2K_s}{\left[1 - P - \frac{K_b}{K_s}\right] + P\frac{K_s}{K_f}} \qquad (2.5)$$

where,

K_s = solid grain bulk modulus,

K_b = solid frame (absent the pore fluid) bulk modulus,

K_f = pore fluid bulk modulus.

For the case of a stationary frame, to which this study is restricted, $\mathbf{u} = 0$. Noting that $\rho_a + \rho_2 = \alpha P \rho_f$, Eq. (2.2) yields, for $\mathbf{u} = 0$:

$$\alpha P \rho_f \frac{\partial^2}{\partial t^2}\mathbf{U} = D\nabla(\nabla \cdot \mathbf{U}) - bF\frac{\partial \mathbf{U}}{\partial t} \qquad (2.6)$$

For a perfectly rigid frame $K_f << K_s, K_b$, and Eq. (2.5) reduces to $D = PK_f$. Recalling also that $b = PR_{DC}$, Eq. (2.6) becomes:

$$\alpha P \rho_f \frac{\partial^2}{\partial t^2} \mathbf{U} = P K_f \nabla(\nabla \cdot \mathbf{U}) - P R_{DC} F \frac{\partial \mathbf{U}}{\partial t} \quad . \tag{2.7}$$

Assuming harmonic time dependence $(e^{j\omega t})$, Eq. (2.7) becomes:

$$-\omega^2 \left(\alpha \rho_f + \frac{R_{DC}}{j\omega} F \right) \mathbf{U} = K_f \nabla(\nabla \cdot \mathbf{U}) \quad . \tag{2.8}$$

From the linearized continuity equation,

$$\nabla \cdot \mathbf{U} = - \frac{\delta \rho_f}{\rho_f} \quad . \tag{2.9}$$

Applying this result and the definition

$$K_f = \rho_f \frac{\delta p}{\delta \rho_f} \tag{2.10}$$

for the bulk modulus to Eq. (2.8) gives:

$$-\omega^2 \left(\alpha \rho_f + \frac{R_{DC}}{j\omega} F \right) \mathbf{U} = -\nabla p \tag{2.11}$$

Defining the complex mass density by

$$\tilde{\rho} = \alpha \rho_f + \frac{R_{DC}}{j\omega} F \quad , \tag{2.12}$$

Eq. (2.9) can be cast in terms of fluid particle velocity $\vec{u} = j\omega \mathbf{U}$ as

$$j\omega \tilde{\rho} \vec{u} = -\nabla p \quad , \tag{2.13}$$

which is in the familiar form of Euler's equation (KFCS, 1982, p. 104), (hereafter the subscript f on $\tilde{\rho}$ will be omitted; it is to be understood).

The real part of Eq. (2.12) is the apparent fluid mass density and the imaginary part is the negative of the apparent flow resistance divided by the angular frequency:

$$\mathrm{Re}\left(\tilde{\rho}\right) = \rho_{eff}(\omega) = \mathrm{Re}\left(\alpha\rho_f + \frac{R_{DC}}{j\omega}F\right) , \tag{2.14}$$

$$\mathrm{Im}\left(\tilde{\rho}\right) = \frac{-R_{flow}(\omega)}{\omega} = \mathrm{Im}\left(\alpha\rho_f + \frac{R_{DC}}{j\omega}F\right) . \tag{2.15}$$

Both Eq. (2.14) and Eq. (2.15) depend on frequency. The normalized complex mass density, $\tilde{\rho}/\rho_f$, is called the complex, or dynamic, tortuosity, $\tilde{\alpha}$, and depends only on the microscopic pore geometry and frequency. In the context of the Biot theory, the microscopic pore geometry is characterized by the three parameters: (intrinsic) tortuosity α, DC flow resistance R_{DC}, and the structure factor δ, which is a scale factor for the argument of the complex universal correction function F. In Biot's original notation, these correspond to the pore size parameter, permeability, and structure factor, respectively (Ogushwitz, 1985, p. 430).

Viscosity of the pore fluid is very important to solid/fluid coupling. A pertinent quantity, therefore, is the viscous penetration depth (δ_v), or skin depth, defined as

$$\delta_v = \sqrt{\frac{2\eta}{\rho_f\omega}} , \tag{2.16}$$

where η is fluid (shear) viscosity. (e.g., $\delta_v = 56\mu$, for water at 20°C and $\omega = 100$ Hz). The relative magnitude of the imaginary and real parts of the complex mass density, and therefore the relative importance of fluid viscosity versus inertia in determining the fluid motion, depends upon the ratio of the viscous penetration depth to a characteristic pore size. If δ_v is small compared to a characteristic pore size, then the motion of the fluid is very similar to that of an inviscid fluid, and independent (of the solid) sound propagation within the fluid is possible. This case is termed the high frequency limit. By contrast, if the viscous penetration depth is large compared to the characteristic pore size, the fluid is essentially locked to the rigid solid frame. In this case, sound cannot propagate independently within the fluid, and it is referred to as the low frequency limit. (Bourbie et al, 1987, p. 86)

Two methods for experimentally determining the complex mass density of a fluid-saturated porous solid are being investigated, termed the direct method and the impedance method. A theoretical description of each follows.

B. DIRECT METHOD

In the so-called direct, or Newton's Second Law, method, the complex mass density $\tilde{\rho}$ is directly obtained from a measurement of the acoustic pressure gradient required to produce a certain (known) acceleration, using Eq. (2.13):

$$\tilde{\rho} = \frac{-\nabla p}{j\omega \vec{u}} \quad . \tag{2.17}$$

The description of how pressure and acceleration are measured is given in the next chapter.

C. IMPEDANCE METHOD

In the impedance method, the complex mass density is indirectly obtained from a measurement of the input electrical impedance (Z_{IN}) of a moving coil transducer as follows, from Wilson (1985, p. 28):

$$Z_{IN} = Z_E + \frac{(Bl)^2}{R_m + R_r + j\omega(M+M_r) + \frac{s}{j\omega}} \quad , \tag{2.18}$$

where;

Bl = transduction coefficient of the driver,

R_m = mechanical resistance of the driver,

R_r = effective mechanical resistance of the fluid,

M = moving mass of the driver,

M_r = effective mass of the fluid,

s = stiffness of the driver,

Z_E = blocked electrical impedance of the driver,

The effective mass, M_r , and the effective mechanical resistance, R_r ,of the fluid, obtained from the imaginary and real parts of Eq. (2.18), respectively, are given by:

$$M_r = \frac{1}{\omega} \mathrm{Im}\left[\frac{(Bl)^2}{Z_{IN} - Z_E}\right] + \frac{s}{\omega^2} - M \quad , \tag{2.19}$$

and

$$R_r = \mathrm{Re}\left[\frac{(Bl)^2}{Z_{IN} - Z_E}\right] - R_m \quad . \tag{2.20}$$

Finally, M_r and R_r are related to ρ_{eff} and R_{flow}, respectively, by

$$\rho_{eff} = \frac{M_r}{PSL} \qquad \text{and} \qquad R_{flow} = \frac{R_r}{PSL} \quad , \tag{2.21}$$

where;

P = the porosity,

S = the cross-sectional area of the chamber,

L = the length of the fluid plug,

PSL = the volume occupied by the fluid.

A description of the apparatus developed to extract the complex mass from impedance measurements using a moving coil loudspeaker follows in the next chapter.

III. EXPERIMENTAL DESIGN, PROCEDURE, AND PRELIMINARY RESULTS

A. BACKGROUND AND PREVIOUS WORK

In Chapter II, theoretical relationships were derived between physically measurable quantities by which the complex moving mass of a fluid contained in a rigid porous solid can be extracted. This chapter describes the design and preliminary results of the two experimental techniques being investigated for this purpose.

For his Master's research, LCDR Grant developed the apparatus for the impedance method, (Grant, 1988), and his work is summarized here. The development of the impedance method was accomplished in two phases: (1) selection and characterization of two matched moving-coil transducers, and (2) design and construction of a test chamber. A pair of Philips model AD062T8 one-inch diameter tweeters, depicted in cross-section in Fig. 2 (Grant, 1988, p. 18), were used as drivers. To ensure oscillatory plug flow of the fluid through the sample of porous material, the pair of transducers were driven in parallel and out-of-phase with respect to each other in a system closed to ambient pressure. To satisfy the rigid frame condition, a massive six inch outer diameter brass test chamber, with a centered 1.5 inch diameter cylindrical cavity, was designed and built as shown in Fig. 3 (Grant, 1988, p. 40). Porous samples are to be housed within a cylindrical metal sleeve, and the sleeve inserted into

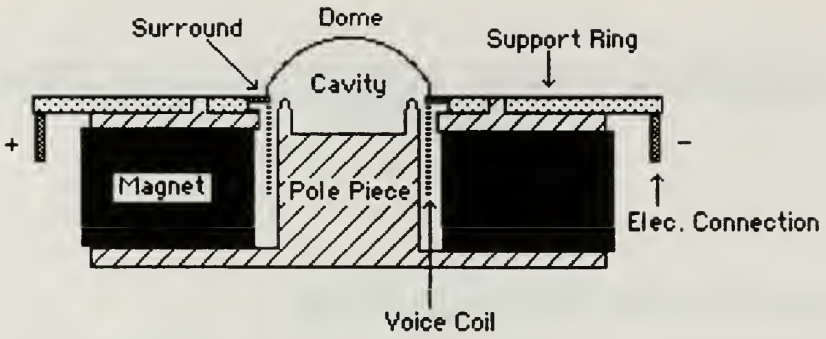

Figure 2. Philips Driver.

the cavity. Overall test chamber length was limited to three inches to avoid acoustic resonances in the experimental frequency range of interest, i.e., below one kilohertz.

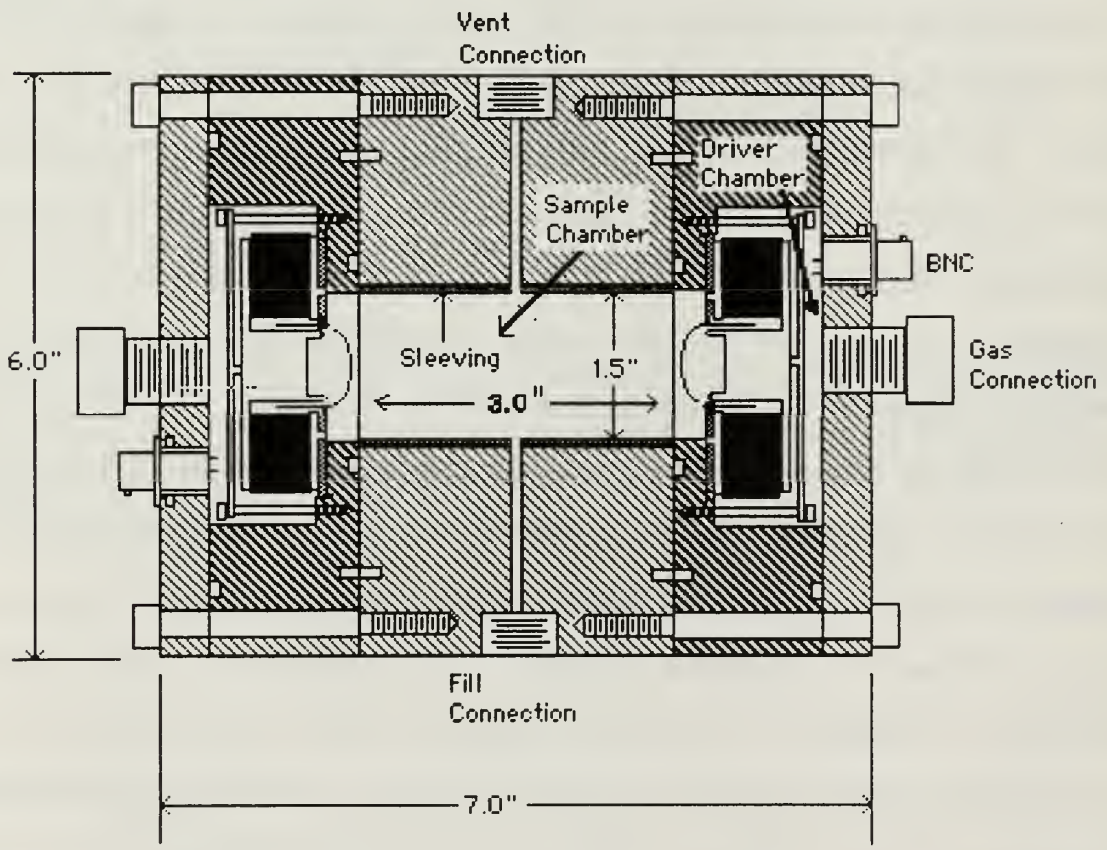

Figure 3. Cutaway View of Impedance Method Apparatus.

In a series of experiments, with the objective to calibrate the apparatus with the sample cavity filled soley with water, LCDR Grant successfully demonstrated that the moving mass load presented to the face of one moving coil transducer could be extracted from its measured input electrical impedance. This required a meticulous and thorough investigation of the five properties of the moving coil driver which appear in Eq. (2.18) (the details of which are presented in Grant,1988). Reported experimental uncertainty in all five quantities was consistently less than 4.5 per cent (Grant, 1988, pp. 21-33). High-precision input electrical impedance measurements were made using a Hewlett-Packard Low Frequency Impedance Analyzer Model 4192 (Hewlett-Packard Corporation, San Jose, Ca.). LCDR Grant concluded that it appeared possible to extract the effective mass with an accuracy of about five percent over a significant portion of the frequency band 100 to 1000 Hz; e.g., Fig. 4 (Grant, 1988, unpublished results).

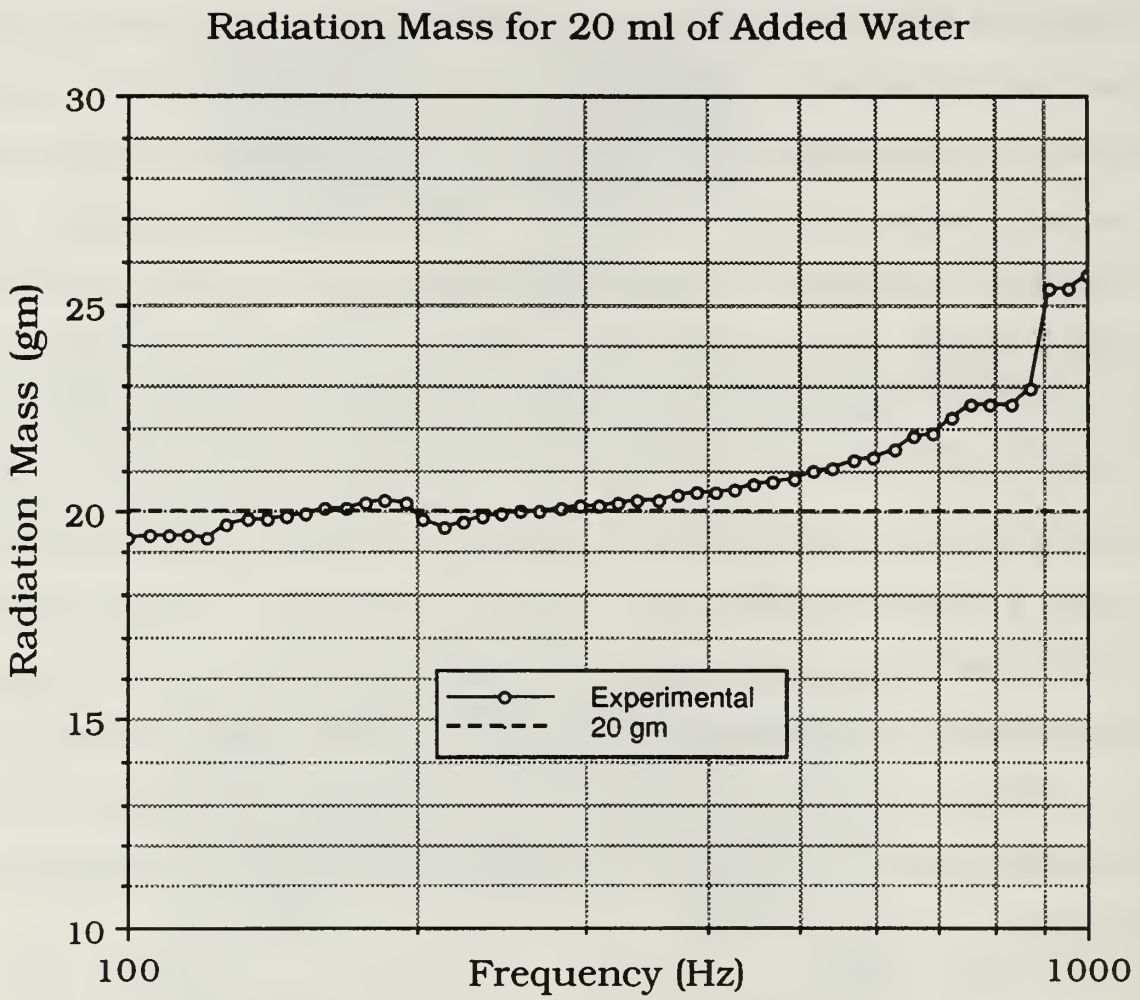

Figure 4. Impedance Method Mass Extraction for 20 ml of Added Water.

B. FURTHER IMPEDANCE METHOD EXPERIMENTS

LCDR Grant's results using the impedance method revealed a systematic error with increasing frequency in the band of interest, as Fig. 4 indicates. The magnitude of this error was found to be greater

for larger added mass. A considerable effort was therefore made in the present investigation to improve the impedance technique. A discussion of the source of the error and a description of the efforts made to correct it follow.

Fig. 5 (Grant, 1988, p. 15) and Fig. 6 (corrected figure from Grant, 1988, p. 14) show the block diagram and lumped element representation of the equivalent electrical circuit for the impedance method. The subscripts M and R indicate the electrical equivalents of the transducer open circuit mechanical impedance and the radiation impedance, respectively, in the mobility analog (KFCS, 1982, p. 360). In this analogy, a greater mechanical or radiation impedance results in a smaller equivalent electrical impedance. For frequencies below one kilohertz, the impedance of the inductance (representing mechanical compliance) is greater than any other element, and this component is largely ignorable. Hence, for increasing frequency, the radiation and mechanical impedances appear more and more as short circuits. Under these conditions, the degree to which the blocked electrical impedance is known determines the precision with which the radiation impedance can be extracted from the measured input electrical impedance.

LCDR Grant realized the blocked electrical impedance cannot be represented as a simple resistor and inductor in series (as in Fig. 6). In fact, a frequency dependent blocked electrical impedance was used to obtain the results shown in Fig. 4. Because it is virtually impossible to completely block a transducer without damaging it, however, the

value of the blocked electrical impedance which Grant used in his analysis was obtained from electrical impedance measurements on a

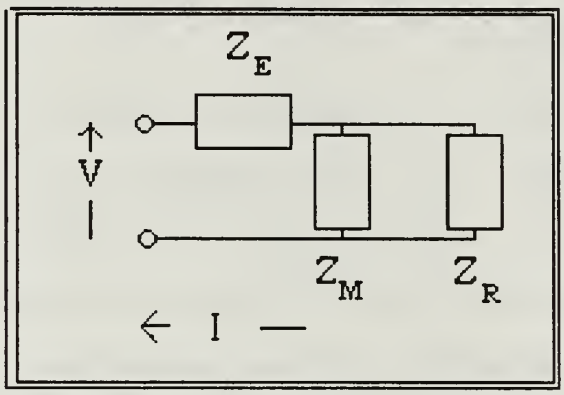

Figure 5. Equivalent Circuit.

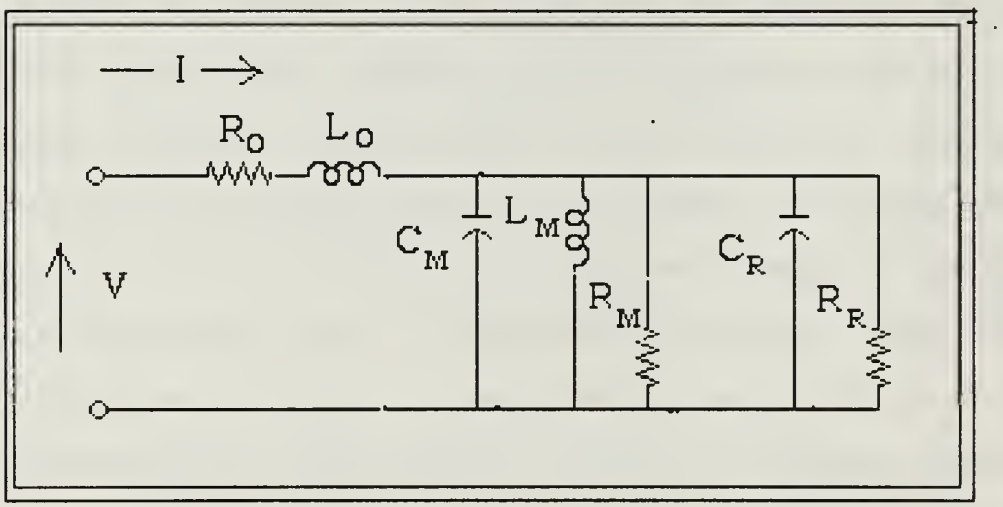

Figure 6. Lumped Element Equivalent Circuit - Mobility Analogy.

similar moving coil transducer which had been completely potted with epoxy (Grant, 1988, p. 22). For the extraction of moving masses of 50 g or so, the blocked electrical impedance must be known with much

more certainty, i.e., for the particular driver being used. Furthermore, because the mechanical resonance of the driver with no added mass occurs at about 1000 Hz, some of the error in the extracted value for the larger masses could be due to insufficient knowledge of the mechanical impedance. In summary, it is believed that extension of the impedance method to successfully extract masses of 50 g or more hinges on knowing the transduction coefficient, mechanical resistance, moving mass of the driver, stiffness of the driver, and the blocked electrical impedance, to a higher degree of accuracy.

The first effort to improve the impedance method involved finding the best values of these parameters, that is, the values which gave the best results for the extracted mass for a collection of known added masses. A computer program was written to control an HP 4192 to measure the input electrical impedance. Impedance measurements were made for added masses of 0 to 100 g in 10 g increments from 10 to 2000 Hz in 10 Hz steps. A grid-search least squares program adapted from Bevington (1969, pp. 208-213) was used to find values of the "known" transducer parameters (Bl, Z_M, Z_E) which minimized the magnitude of the fractional error in the computed and actual radiation impedance ($j\omega M_r$),

$$\left| \frac{\frac{(Bl)^2}{(Z_{IN} - Z_E)} - Z_m}{j\omega M_r} - 1 \right|^2 , \qquad (3.1)$$

and to store the results in a file for use by graphics routines. Seed values for the parameter values were taken from Grant (1988, pp. 13,39). The results showed no significant improvement over Grant's results.

As an alternative attempt to improve the impedance method, the problem of finding the optimum values of the transducer parameters in Eq. (2.18) was re-cast so as to find the complex, frequency dependent transduction coefficient, $\widetilde{Bl}$, that gives the least variance of the mechanical impedance of the transducer extracted from impedance measurements. From Eq. (2.18), the mechanical impedance may be obtained from measurements of input electrical impedance with a mass added, Z_{IN} , and with zero mass added, $Z_{IN,\,NO\,MASS}$, according to:

$$Z_m = \left[\frac{Z_{IN,\,NO\,MASS} - Z_{IN}}{(Bl)^2} + \frac{1}{(Z_m + j\omega M_r)} \right]^{-1} , \qquad (3.2)$$

which has the root

$$Z_m = -\frac{j\omega M_r}{2} + \left[\frac{(j\omega M_r)^2}{4} + \frac{j\omega M_r (Bl)^2}{(Z_{IN,\,NO\,MASS} - Z_{IN})} \right]^{\frac{1}{2}} . \qquad (3.3)$$

This second attempt to obtain better values for the transducer parameters produced results within the experimental error reported by Grant (1988, p. 30) in the band 500 to 1500 Hz. For frequencies greater than 1500 Hz, however, the optimum value of $\widetilde{Bl}$ was unreasonably low, for reasons unknown. Following the disappointing

results of attempts to improve the impedance method using the available apparatus, it was concluded that better results were not likely to be obtained without changing to another driver. Further investigation focused on the development of the direct method, described next.

C. DIRECT METHOD DESIGN

1. Closed System Design

Figure 7 shows a cutaway view of the new apparatus designed and built to extract the complex fluid mass from acoustic pressure and velocity measurements (direct method). The sample chamber is unchanged from the impedance method apparatus. The direct method requires stiff transducers, driven in such a way as to cause the fluid in the sample to oscillate as a plug. For this reason, a "stack" of piezoceramic rings was chosen for the motor element of each driver. Axially polarized Navy Type I lead zirconate-titanate rings, .75 inches in diameter and .25 inches thick, with a .25 inch diameter center hole, were procured (Channel Industries, Inc., Santa Barbara, Ca.). The piezoelectric strain constant in the direction of polarization, d_{33} , was measured for each element using a Berlincourt d_{33} meter (Channel Products, Inc., Chesterland, Oh.). From four selected d_{33}-matched pairs, two nearly identical piezoceramic transducer stacks were assembled by cementing together four rings for each driver.

A piston and surrounding diaphragm assembly seals the cavity at either end of the sample. An impedance head, B&K Model 8001 (Bruel & Kjær, Foster City, Ca.), was positioned between the piezoceramic stack and this assembly. An impedance head is a

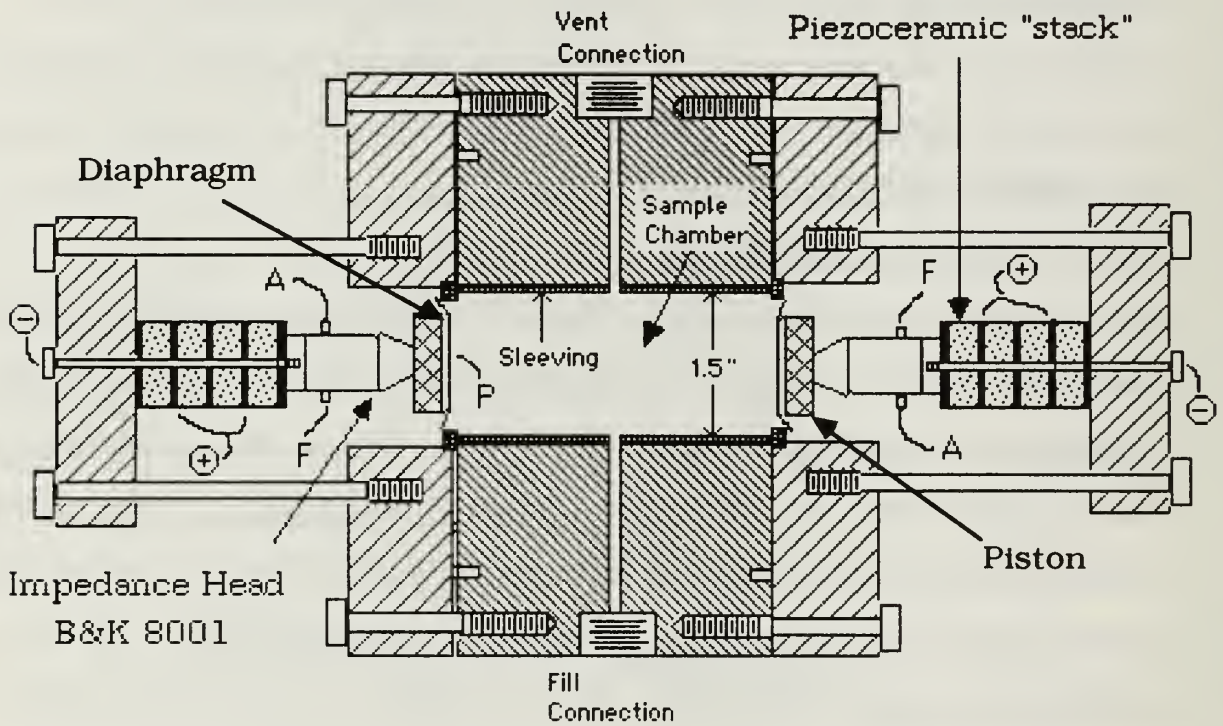

Figure 7. Cutaway View of Direct Method Apparatus.

combination of a force gauge and an accelerometer in one housing. This precision device allowed simultaneous measurement of acceleration and force very close to the driving point of the assembly. The impedance head also secured the threaded end of the compression bolt, providing a static pre-stress on the projector stack.

The opposite end of each stack was cemented to a solid brass slab five inches in diameter and one inch thick.

2. Closed System Acceleration Calibration

The following procedure was developed to match the displacements of the piezoelectric drivers, to ensure plug flow of the fluid in the chamber. The experimental set-up used is depicted in Fig. 8. An approximately constant voltage was simultaneously applied to each stack and the resulting accelerations were compared. This was done from 10 to 2000 Hz in ten-Hz frequency steps. At each frequency, the acceleration of one stack, as measured from the accelerometer in its impedance head, was adjusted to match the other stack's acceleration in magnitude (within +/- 2%) by manually varying the power amplifier. Phase adjustment was not required. A computer program (code listing appears in Appendix B) was written specifically to accomplish the tasks of: (1) measuring and comparing the acceleration magnitude of the two stacks at each frequency, (2) prompting the operator, when necessary, to adjust one stack to achieve a match within the desired tolerance, (3) recording the acceleration and force for each stack, and (4) stepping up the frequency to repeat the process. An HP 9000 Series 300 Computer commanded the HP 3421A Data Aquisition/Control Unit (DAC) and triggered the HP 4192A Low Frequency Impedance Analyzer. With a complete data base of force and acceleration magnitude and phase as a function of frequency, the displacement of the transducers was considered matched and known to within one percent.

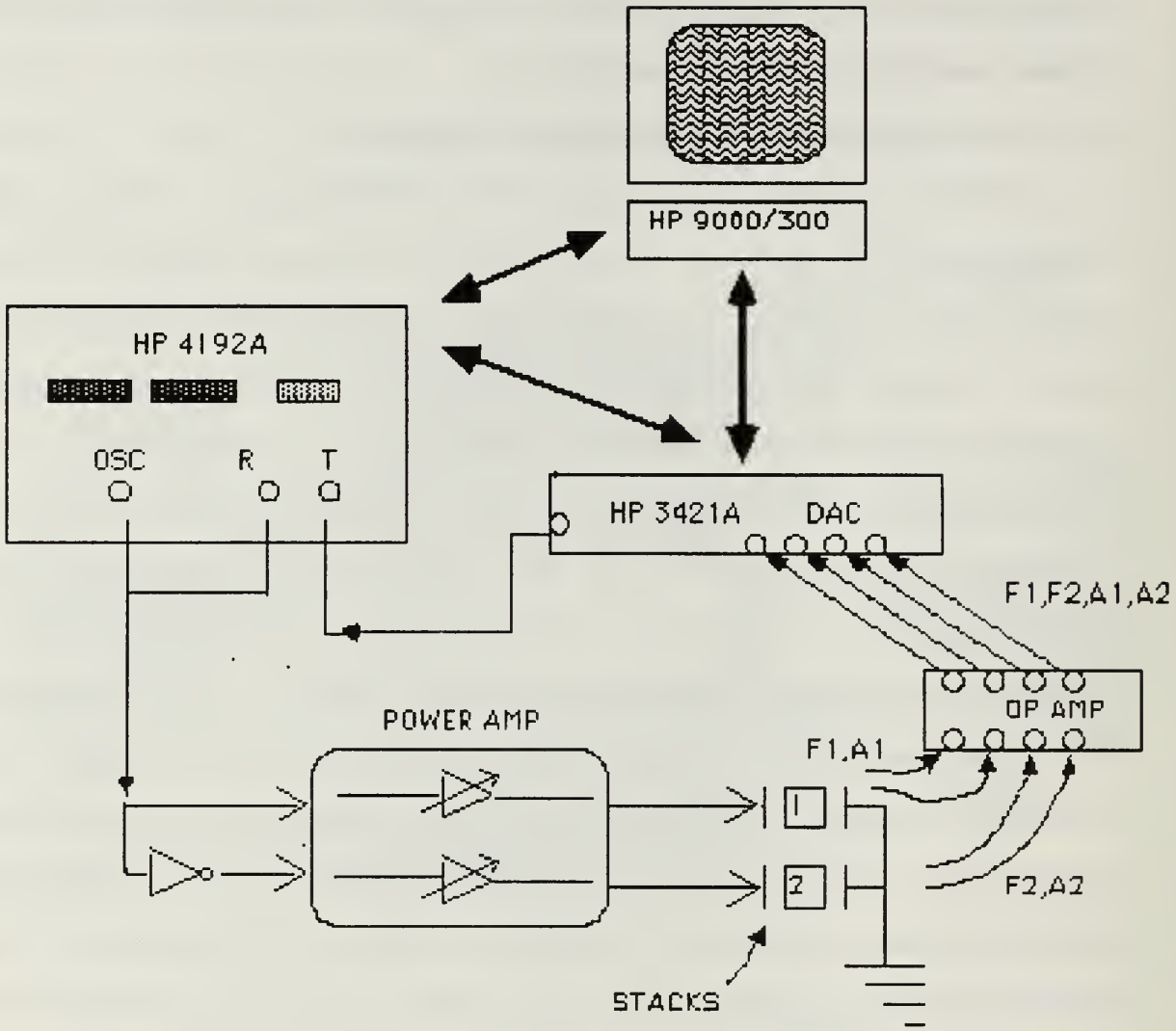

Figure 8. Transducer Calibration Experiment Set-up.

D. DIRECT METHOD EXPERIMENTS

1. Introduction

Several preliminary experiments were conducted using a fluid filled sample chamber with the objective to calibrate the direct

method apparatus. These experiments were performed with a single driver coupled to the test chamber in an "open system" configuration, as illustrated in Fig. 9. In Appendix A, it is shown that the radiation load presented to the open end is neglible in comparison to the moving mass load. Thus, no correction needs to be made to the theory in Chapter II for the open system. With the characteristics of the piezoelectric drivers established, a suitable means to measure the acoustic pressure resulting from the oscillating drive was developed. Finally, a set of calibration experiments was performed, the results of which were used to extract the moving mass of several "unknown" fluid loadings.

2. Measurement of Acoustic Pressure

Referring to Fig. 7, the original intention was to measure the acoustic force on the face of each driver using the impedance head. However, early experiments with various test masses showed that the moving mass could not be seen; i.e., the measured force was dominated by diaphragm stiffness, even though the diaphragm had been made as compliant as practical. To resolve this condition, a means to measure pressure in front of the piston, inside the sample cavity, had to be developed. Relocation of the pressure sensor permitted a stiffer diaphragm to be employed, and thereby reduce the effects of diaphragm flexure on the acoustic pressure in front of the piston. The initial diaphragms were made of 0.001 in. and 0.002 in. thick Mylar, and the final diaphragm was constructed from 0.003 in. thick beryllium copper.

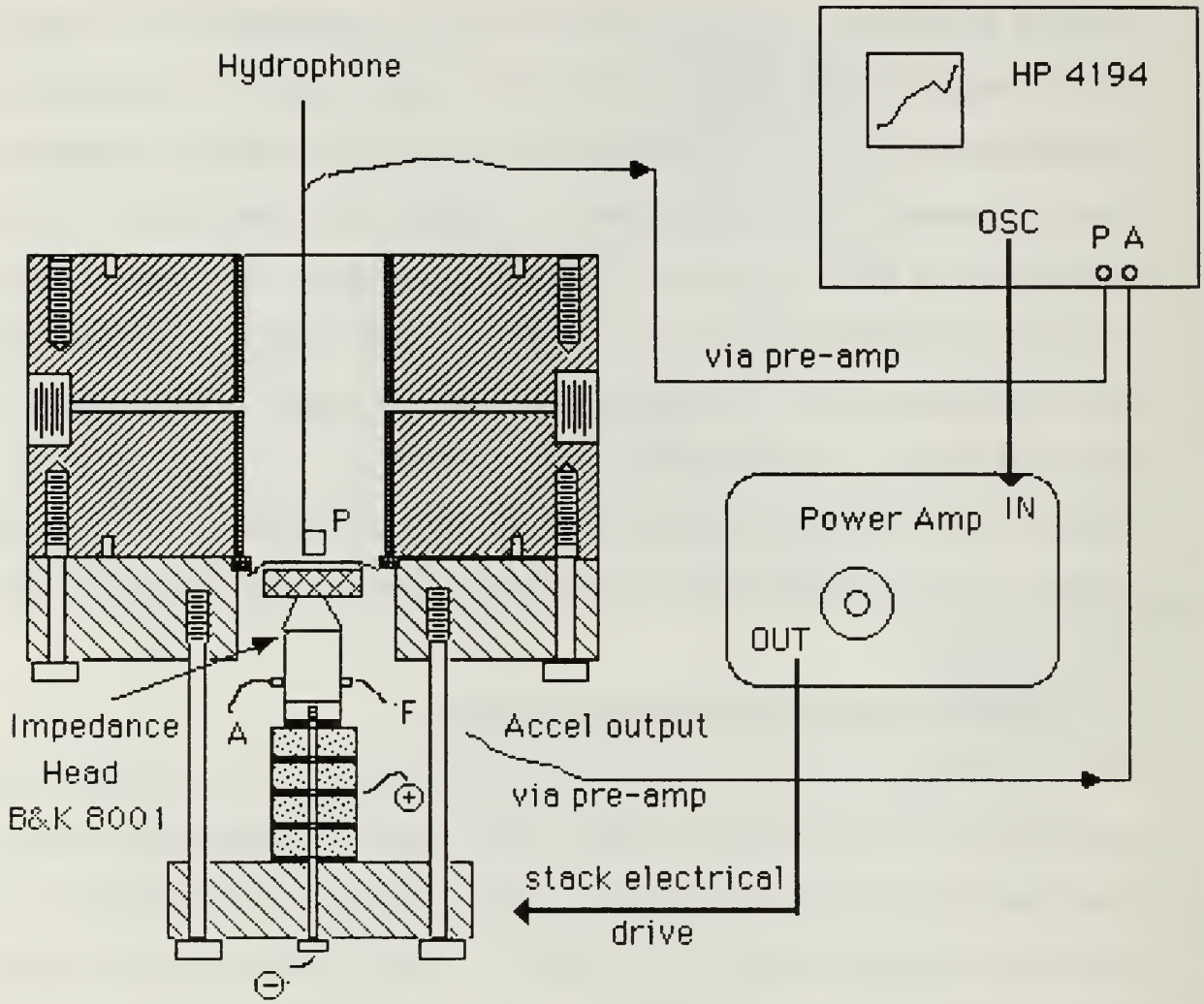

Figure 9. Direct Method Equipment Set-up.

Several alternative methods to measure the pressure inside the sample cavity were tested. Fig. 9 shows the equipment set-up. For these tests, the sample cavity was filled with various amounts of Fluorinert FC-72 non-polar electronic liquid (3M Corporation, St. Paul, Mn.). Fluorinert was used because it is non-conductive and it permits the selection of various viscosities that will be used in later (post

thesis) experimentation. First, a variety of Polyvinylidiene Fluoride (PVF_2 or PVDF) films, ranging from 0.001 in. to 0.01 in. thick (Pennwalt Corporation, Folsom, Ca.), were tried. Each sensor was bonded to the diaphragm. In every case, the resulting voltage response from the pressure sensor was contaminated by resonances of flexural waves in the diaphragm. Next, a similar series of trials was conducted using PVDF sensors suspended in the fluid column in the vicinity of the piston drive. Again, flexural waves dominated the response, in this case propagating in the sensors themselves. A 0.001 in. thick electreted PTFE Teflon sensor was tested, with no improvement over the PVDF series. Finally, a small cylindrical tube piezoceramic hydrophone 6 mm in diameter was tested. The small hydrophone was selected because its lowest frequency resonance is well above the highest frequency of interest in this experiment. While the hydrophone lacked the sensitivity of the PVDF sensors, the measured pressure spectrum over the range 100 to 2000 Hz was substantially improved.

Figure 10, raw data output from the HP 4194 for 80 ml added mass of Fluorinert, is an example of the voltage response of the accelerometer (lower trace) and the hydrophone (upper trace) as a function of frequency, plotted on logarithmic scales. The verticle scale for each trace spans five decades; the minimum and maximum values are listed. The verticle scale markings are for the accelerometer (A) trace. The frequency scale ranges from 30 to 3000 Hz. The signal to noise ratio of the accelerometer output (lower trace)

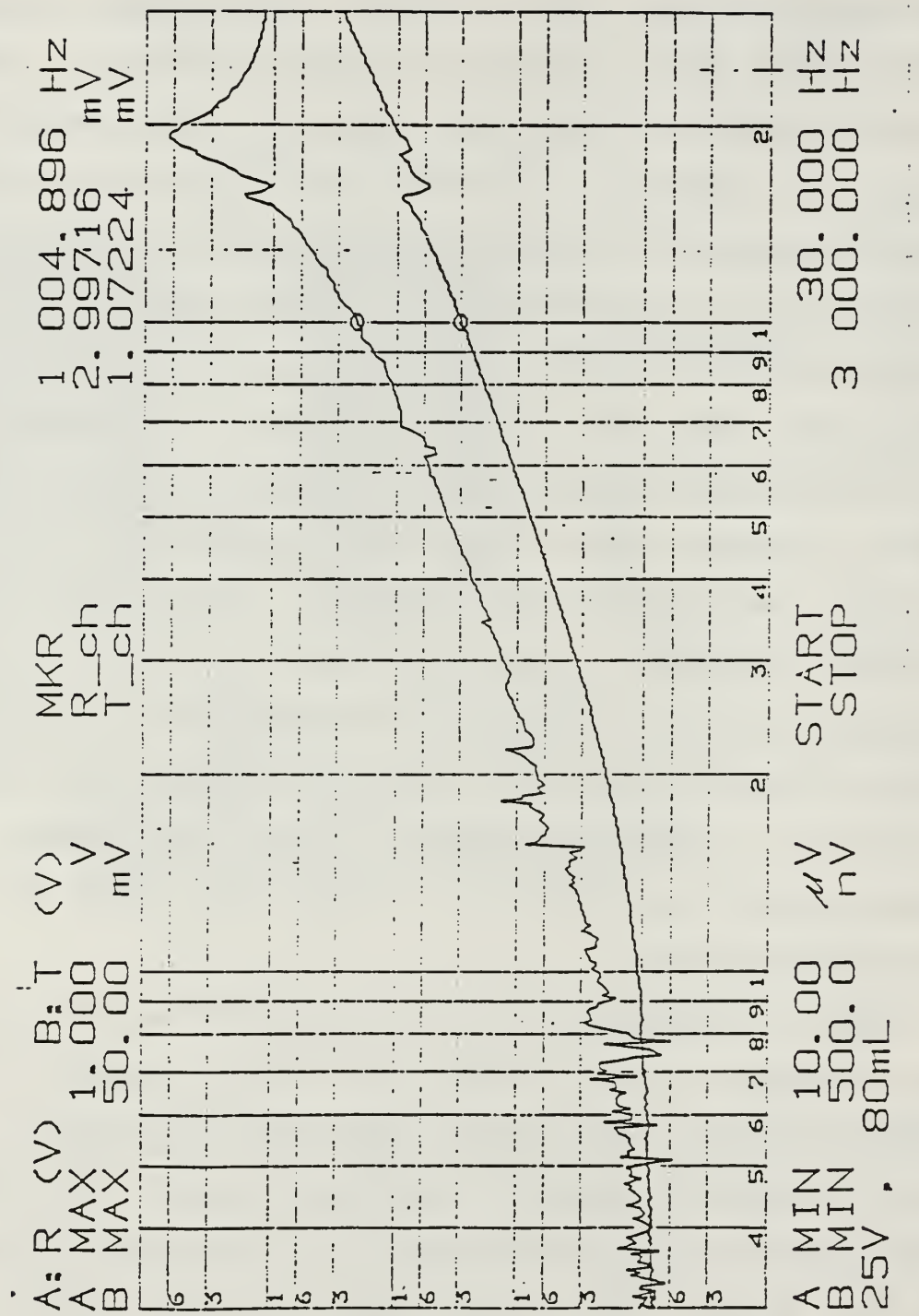

Figure 10. Representative Response of Accelerometer ("A: R" , lower trace) and Hydrophone ("B: T" , upper trace) .

is very high, while the hydrophone output (upper trace) signal to noise ratio is poor at the lower frequencies. The accelerometer output is roughly proportional to f^2 for frequencies above 200 Hz, indicating a constant-displacement drive in this region. Below 200 Hz the acceleration is largely constant. For the most part, the hydrophone output signal is nearly proportional to the accelerometer output, the signature of a mass-like load presented to the driver. The peak in the hydrophone response at about 2000 Hz is a broad, contaminating resonance of unknown origin. As the use of a hydrophone is not compatible with the closed apparatus, it is regarded as an interim solution.

Because of the low signal to noise ratio observed at low frequencies (10-100 Hz), considerable effort went into eliminating noise sources. Though a high driving voltage ($\geq$ 100 V) was desired, the available high voltage amplifier was found to introduce excessive noise into its output. A lower voltage output amplifier, Techron 7520 Power Supply Amplifier (Crown International, Inc., Elkhart, In.), was selected for its low noise output. The Techron amplifier is limited to approximately 25 V rms output voltage. Pre-amplifiers were operated on battery power to avoid 60 Hz harmonic corruption in the pressure and acceleration signals. An exhaustive effort to eliminate ground loops among various equipment (in Fig. 9) proved to be most beneficial.

3. Drive Linearity

Prior to collecting calibration data on the direct method apparatus, a characterization of the drive linearity was performed. Table 3.1 lists the accelerometer and force gauge outputs of the impedance head for applied voltages to the piezoceramic stack of 2V and 20V. The accelerometer and force gauge voltage responses were collected by the gain-phase analyzer. Data at each frequency were also evaluated for the presence of non-linearities using an HP 3580A Spectrum Analyzer. It was observed that the amplitudes of all

TABLE 3.1. DRIVE LINEARITY

Freq. (Hz.)	Acceleration (μV)	
	2 V	20 V
200	16.5	162
498	65.5	651
1005	246	2457
2005	1023	10230
Freq. (Hz.)	Force (mV)	
	2 V	20 V
200	5.94	59.4
498	5.89	58.9
1005	5.67	56.7
2005	4.74	47.4

harmonics were at least 30 dB below that of the fundamental driving frequency. As a result, it was concluded that the drive is linear.

4. Calibration of the Direct Method Apparatus

The objective of this final experiment was to obtain a set of calibration data for the apparatus which can be subsequently used to determine the unknown moving mass of a fluid contained in a rigid porous solid. An evaluation of the calibration data set was made possible by a comparison with results for known moving masses of fluid. For a nearly constant drive voltage of 25 V, calibration pressure and acceleration measurements were recorded as a function of frequency using the equipment in Fig. 9. Fluorinert was added in increments of 10 ml , from 50 to 90 ml (the specific gravity of Fluorinert FC-72 is 1.68, the sound speed is 525 m/s). As with previous experiments using water, the viscous penetration depth of FC-72 is much smaller than the chamber sleeve (pore) radius; e.g., at 100 Hz, $\delta_{FC\text{-}72} \cong 100\,\mu$. Plots were obtained for pressure and acceleration for the band 20 to 2000 Hz at each 10 ml increment for qualitative analysis, e.g., Fig. 10. Because a broad resonance around 2000 Hz dominated the upper end of the frequency range, concurrent recordings of pressure and acceleration were taken at regular frequency intervals only over the range 100 to 1000 Hz. The data were collected using long time integration and 16 averages (features of the HP 4194), and the resulting calibration data set was stored in table format (a convenient function of the HP 4194).

Drive voltage uncertainty was less than 2% and added volume uncertainty was less than 4%. Most of the added mass error was attributed to evaporation of Fluorinert FC-72 at room temperature. Since extracted mass is a quotient of the two experimentally measured values, per Eq. (2.17), each known to better than 4%, overall experimental error is less than 6%.

Using 60 and 80 ml data as the calibration control set, extraction of the moving mass for 50, 70, and 90 ml were accomplished at the selected frequencies from the following interpolation/extrapolation formula:

$$\text{Volume}_{\text{EXTRACTED}}(\omega) = 60 + (80 - 60)\left[\frac{\left(\frac{V_p}{V_a}\right)_X - \left(\frac{V_p}{V_a}\right)_{60}}{\left(\frac{V_p}{V_a}\right)_{80} - \left(\frac{V_p}{V_a}\right)_{60}}\right], \qquad (3.4)$$

where, for a given mass loading and frequency: V_p is the output voltage of the pressure sensing hydrophone and V_a is the output voltage of the accelerometer. The results of the extraction of the volume of moving mass, Fig. 11, are well within experimental error over most of the decade in frequency, 100 to 1000 Hz, and constitute a successful calibration of the direct method apparatus. Significantly, the ability to discern the volume of unknown added mass, or the resolution in ml, is 5% or about 4 ml.

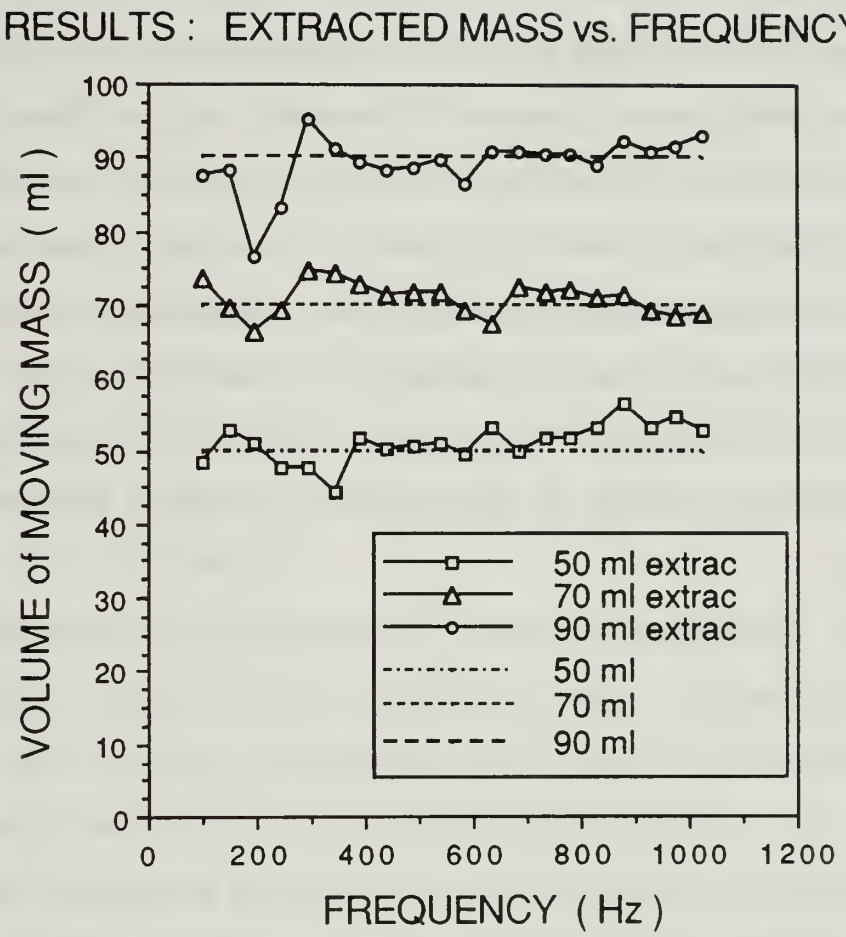

Figure 11. Calibration Results for the Direct Method.

IV. INTERPRETATION OF RESULTS

A. COMPARISON OF TECHNIQUES

It is important to compare the preliminary calibration results from the two methods and identify the more promising technique for future investigations with porous media of unknown complex mass. The impedance method is procedurally very easy to perform with the HP 4194 Impedance/Gain-Phase Analyzer. However, because the extraction of moving mass is indirect, the impedance method is a technique which requires much finesse; a precise knowledge of the properties of the transducer is essential. What the direct method lacks in experimental ease is made up in its direct extraction of complex mass.

Apparatus prototypes for both techniques were developed and employed successfully. The preliminary results of the impedance method, represented by Fig. 4, are comparable to those of the direct method, Fig. 11. Five per cent uncertainty in extracted mass over most of the frequency band 100 to 1000 Hz was established in both techniques. However, because the impedance method is plagued by a systematic deviation in extracted mass at higher frequencies, which increases in magnitude with increasing added mass, it is doubtful that moving masses greater than 50 g can be extracted using this technique with the present moving coil driver. The direct method exhibits no such error. Uncertainty in applying the direct method can

further be reduced by refinement of the design of the piston and surrounding diaphragm to reduce the effect of flexural waves.

B. THE PREFERRED METHOD

Based on the preliminary results of both experimental techniques to date, the use of the direct method for further investigation is recommended. While there is room for improvement in the apparatus of both techniques, the impedance method is limited by a driver that appears unsuitable for extraction of moving masses greater than 50 g. Conversely, it has been demonstrated that it is possible to extract a moving mass of approximately the value expected for fluid-filled porous solid samples ($\approx$ 100 g) with a resolution of several percent using the direct method.

V. CONCLUSIONS

An experimental apparatus was developed by which the complex mass of a viscous fluid contained in a rigid porous solid can be directly extracted from acoustic pressure and acceleration measurements.

Several preliminary experiments were conducted to verify the ability to extract the value of a known mass of fluid. The results for the extracted mass were accurate to within five per cent of known values over most of the frequency range 100 to 1000 Hz.

A comparison of the preliminary results of the two techniques of obtaining complex mass demonstrated that the direct method was most suitable for use in further work investigating porous solid geometries.

APPENDIX A OPEN SYSTEM THEORY

Calibration of both the direct and impedance methods was accomplished using the open system, single transducer/test chamber set-up of Fig. 9 (direct method) and Fig. 12 (impedance method). The effect of the radiation load presented to the open end on the load presented to the driver needs to be examined. Ignoring the radiation load for the moment, in the long wavelength limit, the impedance presented to the face of the driver by the liquid in the chamber alone is (Grant, 1988, pp. 8-10),

$$Z_{rad_{DRIVER}} = Z_{rad_{LIQ}} = j\omega M_r \quad , \tag{A.1}$$

where M_r is the mass of the liquid. Since the particle velocity is the same at the top and bottom of the liquid in the low frequency limit, the impedance seen by the driver is just the sum of the above, Eq. (A.1), and that of the radiated sound wave in air:

$$Z_{rad_{DRIVER}} = Z_{rad_{LIQ}} + Z_{rad_{AIR}} \quad . \tag{A.2}$$

Substituting Eq. (A.1) for $Z_{rad_{LIQ}}$ and the appropriate expression for $Z_{rad_{AIR}}$, assuming the worst case of ka = 1, into the right side of Eq. (A.2) gives:

$$Z_{rad_{DRIVER}} = j\omega M_r + \rho c S \quad , \tag{A.3}$$

where S is the area of the sample at the fluid/air boundary. Since

$$\frac{|\rho c S|}{|j\omega M_T|} << 1 \qquad \text{(A.4)}$$

for the stated experimental conditions and dimensions, Eq. (A.3) may be approximated as:

$$|Z_{rad_{DRIVER}}| \cong \omega M_T = |Z_{rad_{LIQ}}| \,. \qquad \text{(A.5)}$$

Thus, the theory in Chapter II does not need to be modified for the open system.

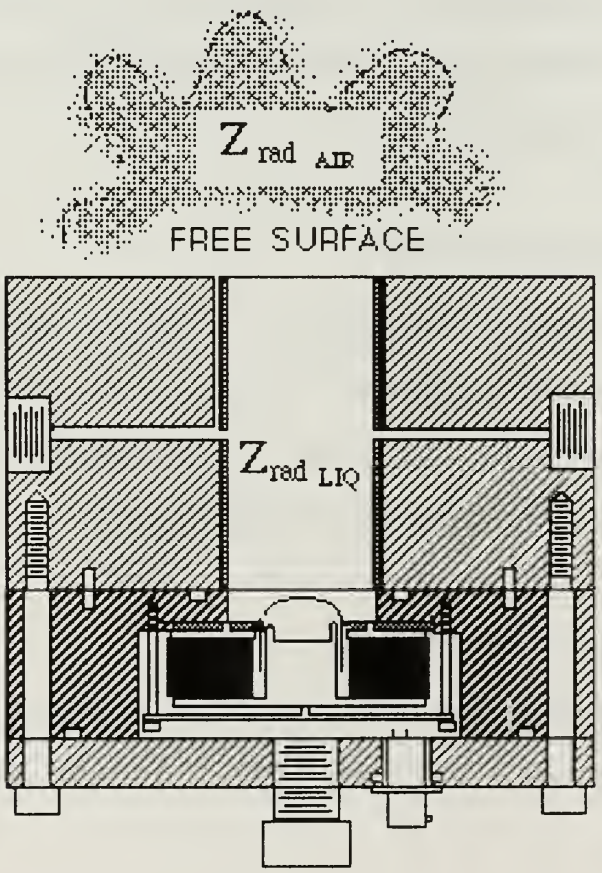

Figure 12. Single Transducer/Test Chamber Open System.

APPENDIX B TRANDUCER CALIBRATION PROGRAM

```
10    !*****************************************************************
20    !                          CALDUCER
30    !*****************************************************************
40    !
50    !   DIRECT MEASUREMENT METHOD - COMPLEX MASS DENSITY
60    !                     CALIBRATION PROGRAM
70    !
80    !*****************************************************************
90    !*****************************************************************
100   !
110   CONTROL 1,12;0                                  ! Softkeys ON
120   PRINTER IS CRT
130   PRINT USING "@"
140   PRINT USING "//"
150   !
160   !      written by R. A. MIRICK,      last update 20 NOV 89
170   !
180   DISP "Ensure Power ON to Analyzer, DAC, and all ancillary equipment"
190   WAIT 5.
200   PRINT " "
210   DISP "Press CONTINUE when ready ..."
220   PAUSE
230   DISP " "
240   !*****************************************************************
250   !  INITIAL CONDITIONS
260   !*****************************************************************
270   OPTION BASE 1
280   INTEGER I,Npts
290   DIM Freq_hz(200),Accel7mks(200),Accel7deg(200),Accel8mks(200)
300   DIM Accel8deg(200),Force9mks(200),Force9deg(200),Force10mks(200)
310   DIM Force10deg(200),Ref_indbv(200),Bminus_a7magdb(200)
320   DIM Bminus_a8magdb(200),Accel_7magv(200),Accel_8magv(200)
330   DIM Bminus_a9magdb(200),Bminus_a10mgdb(200),Force_9magv(200)
340   DIM Force_10mgv(200)
350   MASS STORAGE IS ":,700,1"
360   DEG
370   Osc_level=.5                              ! Volts rms
380   ASSIGN @Analyzer TO 717                   ! Analyzer = HP4192A
390   ASSIGN @Dac TO 709                            ! DAC = HP3421A
400   CLEAR @Analyzer
410   CLEAR @Dac
420   WAIT 3.
430   STATUS @Analyzer;Srq_statbyte
440   IF Srq_statbyte=64 OR Srq_statbyte>64 THEN    ! Error exists!
450        DISP "INPUT ERROR..."
460        GOTO 1610                                ! TERMINATE
470   END IF
480   !
```

```
510   !-----------------------------------------------------------------
520   !*****************************************************************
530   !  CALIBRATION PROCEDURE
540   !*****************************************************************
550   OUTPUT @Analyzer;"OL";Osc_level;"EN"
560   OUTPUT @Analyzer:"N2T2V1"          ! External trigger, measure in dBV,
570                                      !      AVERAGE ON
580   OUTPUT @Analyzer;"EX"
590   WAIT 4.
600   Npts=0
610   FOR I=10 TO 2000 STEP 10             ! I= Frequency in Hz
620        Npts=Npts+1
630        Freq_khz=I/1000.
640        OUTPUT @Analyzer;"FR";Freq_khz;"EN"    ! Spot frequency set to I Hz
650      ! WAIT 1.                 ! Allow settling time for impedance follower's
660                                 !      operational amplifier
670        BEEP 3011.,.5
680        DISP "FREQUENCY IS ",I," Hz"
690        WAIT 2.
700        OUTPUT @Analyzer:"A6N2V1"           ! Function: measure REF input
710        OUTPUT @Analyzer:"EX"               ! Trigger command
720        WAIT 1.                             ! Take advantage of AVERAGE-ing
730        ENTER @Analyzer:Ref_indbv(Npts)
740        DISP "Reference input is ",Ref_indbv(Npts)," dBV"
750        WAIT 4.
760       !DISP "Observe input on Oscope  "    ! Ensure signal is not clipped
770        OUTPUT @Analyzer:"A5N2V1"           ! Function: measure TEST input
780        OUTPUT @Dac:"OPN"                       ! Open all relays
790        OUTPUT @Dac:"CLS7"
800        WAIT .01                                ! Ensure relay closure
810        OUTPUT @Analyzer;"EX"
820        WAIT 1.
830        ENTER @Analyzer:Bminus_a7magdb(Npts),Accel7deg(Npts)
840        OUTPUT @Dac:"OPN7"
850        OUTPUT @Dac:"CLS8"
860        WAIT .01
870        OUTPUT @Analyzer:"EX"
880        WAIT 1.
890        ENTER @Analyzer:Bminus_a8magdb(Npts),Accel8deg(Npts)
900        OUTPUT @Dac;"OPN8"
910     ! - - -     dBV to Volts   - - - !
920        Accel_7magv(Npts)=10.^((Bminus_a7magdb(Npts)+Ref_indbv(Npts))/10.)
930        Accel_8magv(Npts)=10.^((Bminus_a8magdb(Npts)+Ref_indbv(Npts))/10.)
940     ! - - -     Volts to m / sec^2   !
950        Accel7mks(Npts)=Accel_7magv(Npts)*309.6
960        Accel8mks(Npts)=Accel_8magv(Npts)*324.7
970     !- - - NOTE :  THIS CONVERSION APPLIES ONLY TO IH# 9287 & 9315  - - - !
980        Cal_diff=Accel7mks(Npts)/Accel8mks(Npts)
990        DISP "         Acceleration ratio is ",Cal_diff
1000    !
        !                                  ---------------------------------
```

```
1010    !-----------------------------------------------------
1020    !
1030       WAIT 2.
1040       IF Cal_diff>1.1 OR Cal_diff<.9 THEN          ! Accuracy of procedure
1050            DISP " WARNING... Acceleration ratio is ",Cal_diff
1060            WAIT 4.
1070            INPUT "Do you wish to try again? Y/N  ",Answ$
1080            IF Answ$="Y" OR Answ$="y" THEN GOTO 780
1090       END IF
1100       OUTPUT @Dac:"OPN8"
1110       OUTPUT @Dac:"CLS9"
1120       WAIT .01
1130       OUTPUT @Analyzer:"EX"
1140       WAIT 1.
1150       ENTER @Analyzer:Minus_a9magdb(Npts),Force9deg(Npts)
1160       OUTPUT @Dac:"OPN9"
1170       OUTPUT @Dac:"CLS10"
1180       WAIT .01
1190       OUTPUT @Analyzer:"EX"
1200       WAIT 1.
1210       ENTER @Analyzer:Minus_a10mgdb(Npts),Force10deg(Npts)
1220       OUTPUT @Dac:"OPN10"
1230    ! - - -    dBV to Volts    - - - !
1240       Force_9magv(Npts)=10.^((Minus_a9magdb(Npts)+Ref_indbv(Npts))/10.)
1250       Force_10mgv(Npts)=10.^((Minus_a10mgdb(Npts)+Ref_indbv(Npts))/10.)
1260    ! - - -    Volts to Newtons - - !
1270       Force9mks(Npts)=Force_9magv(Npts)*2.525
1280       Force10mks(Npts)=Force_10mgv(Npts)*2.538
1290    !- - - NOTE :  THIS CONVERSION APPLIES ONLY TO IH# 9287 & 9515  - - - !
1300       Freq_hz(Npts)=I
1310    NEXT I
1320    STATUS @Analyzer:Srq_statbyte
1330    IF Srq_statbyte=64 OR Srq_statbyte>64 THEN      ! Error exists!
1340         DISP "INPUT ERROR..."
1350         GOTO 1610                                  ! TERMINATE
1360    END IF
1370    !
1380    !-----------------------------------------------------------------------
```

```
1400  !*************************************************************
1410  !   OUTPUT
1420  !*************************************************************
1430  INPUT "Enter the OUTPUT file name...",Name$
1440  CREATE BDAT Name$,1800,8
1450  ASSIGN @File_name TO Name$
1460  FOR I=1 TO Npts
1470       OUTPUT @File_name;Freq_hz(I)
1480       OUTPUT @File_name;Accel7mks(I)
1490       OUTPUT @File_name;Accel7deg(I)
1500       OUTPUT @File_name;Accel8mks(I)
1510       OUTPUT @File_name;Accel8deg(I)
1520       OUTPUT @File_name;Force9mks(I)
1530       OUTPUT @File_name;Force9deg(I)
1540       OUTPUT @File_name;Force10mks(I)
1550       OUTPUT @File_name;Force10deg(I)
1560  NEXT I
1570  ASSIGN @File_name TO *
1580  !*************************************************************
1590  !  TERMINATE
1600  !*************************************************************
1610  PRINT USING "@"
1620  PRINT USING "///"
1630  PRINT "Program conclusion..."
1640  PRINT
1650  BEEP 406,.5
1660  BEEP 651,.5
1670  BEEP 895,.5
1680  BEEP 162,1.0
1690  END
```

REFERENCES

Akal, T., and Berkson, J. M., *Ocean Seismo-Acoustics*, pp. 1-915, Plenum Press, 1986.

Baker, S. R., *Sound Propagation in a Superfluid Helium Filled Porous Solid: Theory and Experiment*, PhD Dissertation, Department of Physics, University of California at Los Angeles, July 1986.

Bedford, A., Costley, R. D., and Stern, M., "On the Drag and Virtual Mass Coefficients in Biot's Equations," *Journal of the Acoustical Society of America*, v. 76, pp. 1804-1809, 1984.

Bevington, P. A., *Data Reduction and Error Analysis for the Physical Sciences*, pp. 208-214, McGraw-Hill, Inc., 1969.

Biot, M. A., "Theory of Propagation of Elastic Waves in Fluid Saturated Porous Solids: I. Low Frequency Range," *Journal of the Acoustical Society of America*, v. 28, p. 168, 1956.

Biot, M. A., "Theory of Propagation of Elastic Waves in Fluid Saturated Porous Solids: II. High Frequency Range," *Journal of the Acoustical Society of America*, v. 28, p. 179, 1956.

Biot, M. A., "Generalized Theory of Acoustic propagation in Porous Dissipative Media," *Journal of the Acoustical Society of America*, v. 34, pp. 1254-1264, 1962.

Bourbie, T., Coussy, O., and Zinszner, B., *Acoustics of Porous Media*, p. 86, Gulf Publishing Company, 1987.

Grant, S. D., *Development of a Compact Apparatus for Determining Complex Parameters of Fluid Filled Porous Solids by Impedance Techniques*, Master's Thesis, Naval Postgraduate School, Monterey, California, September 1988.

Hamilton, E. L., "Geoacoustical Models of the Sea Floor," *Physics of Sound in Marine Sediments*, pp. 181-221, Plenum Press, 1974.

Hampton, L., *Physics of Sound in Marine Sediments*, pp. 1-567, Plenum Press, 1974.

Hovem, J. M., "Attenuation of Sound in Marine Sediments," *Bottom-Interacting Ocean Acoustics*, p. 2, Plenum Press, 1980.

Johnson, D. L., Koplik, J., and Dashen, R., "Theory of Dynamic Permeability and Tortuosity in Fluid-Saturated Porous Media," *Journal of Fluid Mechanics*, v. 176, p. 379, 1987.

Kibblewhite, A. C., "Attenuation of Sound in Marine Sediments: A Review with Emphasis on New Low Frequency Data," *Journal of the Acoustical Society of America*, v. 86, pp. 716-738, 1989.

Kinsler, L. E., Frey, A. R., Coppens, A. B., and Sanders, J. V., *Fundamentals of Acoustics*, pp. 104,360, John Wiley & Sons, Inc., 1982.

Kuperman, W. A., and Jensen, F. B., *Bottom-Interacting Ocean Acoustics*, pp. 1-717, Plenum Press, 1980.

Ogushwitz, P. R., "Applicability of the Biot Theory: I. Low Porosity Materials," *Journal of the Acoustical Society of America*, v. 77, p. 429, 1985.

Plona, T. J., and Johnson, D. L., "Acoustic Properties of Porous Systems: I. Phenomenological Description," *Physics and Chemistry of Porous Media*, p. 89, American Institute of Physics, 1984.

Stoll, R. D., "Acoustic Waves in Saturated Sediment," *Physics of Sound in Marine Sediments*, pp. 19-39, 1974.

Stoll, R. D., "Marine Sediment Acoustics," *Journal of the Acoustical Society of America*, v. 77, p. 1789, 1985.

Stoll, R. D., "Acoustic Waves in Marine Sediments," *Ocean Seismo-Acoustics*, pp. 417-434, Plenum Press, 1986.

Tolstoy, I., and Clay, C. S., *Ocean Acoustics*, p. 8, American Institute of Physics, 1987.

Urick, R. J., *Sound Propagation in the Sea*, p. 11-1, Peninsula Publishing, 1982.

Wilson, O. B., *An Introduction to the Theory and Design of Sonar Transducers*, p. 28, U. S. Government Printing Office, 1985.

INITIAL DISTRIBUTION LIST

		No. Copies
1.	Defense Technical Information Center Cameron Station Alexandria, VA 22304-6145	2
2.	Library, Code 0142 Naval Postgraduate School Monterey, CA 93943-5002	2
3.	Professor S. R. Baker (Code 61Ba) Naval Postgraduate School Monterey, CA 93943-5000	8
4.	Professor O. B. Wilson (Code 61Wl) Naval Postgraduate School Monterey, CA 93943-5000	2
5.	Professor A. A. Atchley (Code 61Ay) Naval Postgraduate School Monterey, CA 93943-5000	1
6.	Professor K. E. Woehler (Code 61Wh) Naval Postgraduate School Monterey, CA 93943-5000	1
7.	LCDR. R. A. Mirick, USN 6 Robandy Road Andover, MA 01810	2

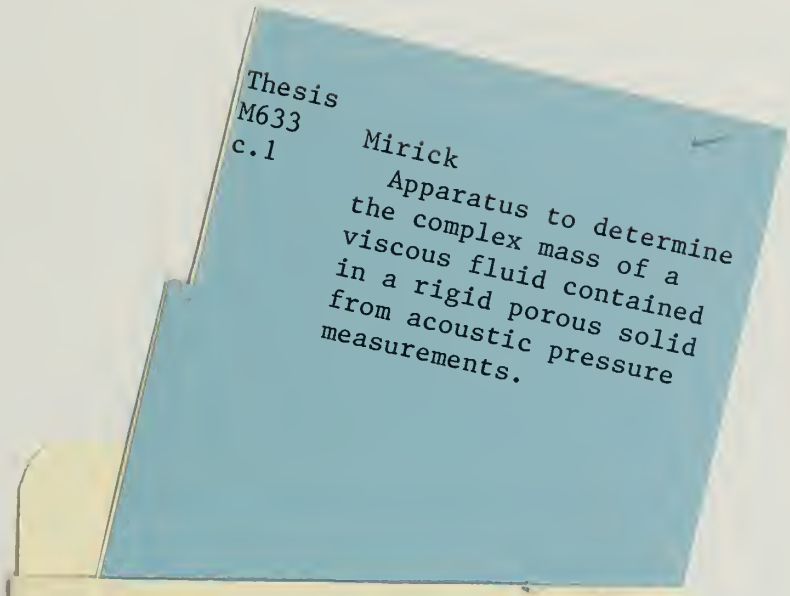

Thesis
M633
c.1
Mirick
Apparatus to determine the complex mass of a viscous fluid contained in a rigid porous solid from acoustic pressure measurements.